Journal of Chemical Technology and Metallurgy, 57, 5, 2022, 1060-1070

NIOBIZED LAYERS PRODUCED ON TI-6AL-4V ALLOY AND THEIR MECHANICAL PROPERTIES

Alaeddine Kaouka[1], Mourad Keddam[2], Abdelhalim Zoukel[3]

[1]*Laboratoire de Sciences Appliquées et Didactiques*
Ecole Normale Supérieure de Laghouat, Algeria
[2]*Laboratoire de Technologie des Matériaux*
USTHB BP 32 El-Alia 16111 Algiers, Algeria
[3]*Laboratoire Physico-chimie, Ammar Telidji University*
BP37G 03000 Laghouat, Algeria
E-mail: a.kaouka@lagh-univ.dz

Received 25 January 2022
Accepted 23 March 2022

ABSTRACT

In this work, the microstructural and mechanical properties of treated Ti-6Al-4V alloy were investigated. Ekabor II boriding first treatment was carried out in this alloy for the formation of boride layers, and then a powder technique treatment with niobium was realized as a second treatment to form niobized layers. Scanning Electron Microscopy, Optical Microscopy, and X-ray diffraction were used to observe the obtained microstructures. It revealed that titanium alloy treated is composed of α" lamellar and β phase stabilized by niobium. Besides, the microstructure of Ti-6Al-4V alloy is composed of α + β phases. The microstructure contained two layers, which are differed in phase composition. The outer layer contained niobium (Ti Nb), while the inner layer contained a mixture of titanium borides (TiB_2 and TiB). The presence of niobium caused an increase in the micro hardness of the outer layer in comparison to the sample without niobium. The average values of indentation Vickers hardness (HV) obtained were equal to 1728 ± 50. Niobium presence has remarkable influence on the mechanical properties of inner layer of titanium borides (TiB_2 and TiB). Moreover, the fracture toughness of the phase composition of the treated area was investigated.

Keywords: niobium, Ekabor II boriding, titanium Ti-6Al-4V alloy, mechanical properties.

INTRODUCTION

Boriding is well known as a surface treatment, where boron is diffused into the surface of the substrate, in order to improve the mechanical characteristics such as microhardness, abrasive wear resistance, and corrosion resistance in engineering components of substrates [1 - 4]. Substrates can be ferrous materials like iron (steels and cast iron), which generally have a low and medium steel alloy [5 - 7, 14, 16, 17], and non-ferrous materials such as, cobalt, nickel [8 - 10] and titanium alloys [11 - 14]. Boriding can be done in different media such as solid (powders or pack-past) [5, 7, 11, 15], liquid [6, 16], gaseous [17], and plasma [13, 14]. However, the commercial Ekabor II powder is widely used due to its simplicity and cleanness obtained samples. Therefore, the boriding process is a suitable treatment, that causes enhancement of some mechanical properties.

Thus, different works have been approved on boriding treatment. The boriding process was performed in basic to moderated activation (BF_3 or SiO_2) and boron carbide B_4C [4, 16]. X-ray analysis and mechanical characterization (micro hardness, fracture toughness, and wear tests) were realized to describe the phase nature, morphology, and adherence of the boride layers produced on the substrate. A single-phase acicular layer of Fe_2B is formed and it can be applied to alloy steels. The micro hardness value of boride steels was equal to around 1450 - 1850 HV, which presented good adhesion to the steel alloys as long as the boride layers were composed of single Fe_2B [5]. The micro hardness is around 1760 HV for liquid boriding in a slurry salt liquid bath comprising about 20 % ferrosilicon, 20 % boric acid, and 60 % borax, forming both FeB and Fe_2B

phases [6]. Micro hardness of the boride layer is in the range 1542.6 HV - 2228.7 HV of on surface Inconel 600 alloy via gas boriding [17], and 2867.6 HV for titanium via plasma paste boriding [13]. Many authors studied the growth kinetics of boride layers for different kinds of steels [6, 7, 11] and titanium [12 - 14, 23, 24]. Plasma boriding leads to the formation of TiB_2 and TiB on the surface of pure titanium as well as of Ti-6Al-4V alloy.

The parabolic growth constants were calculated and the boron diffusion coefficients were determined in the literature [14]. Titanium alloys compared with stainless steel and cobalt-chromium alloys have good properties, such as good biocompatibility, good corrosion resistance, high specific strength, low density, and low elastic modulus. It has a wide range of applications in the aerospace and orthopedic fields.

However, titanium alloy Ti–6Al–4V has a lower rigidity and higher cost than other implant materials such as stainless steels or cobalt-chromium alloy. It has been limited in some practical applications at high temperatures above 820°C, in aeronautics, or even in biomedicine. Thus, titanium alloys need to develop their performances, in terms of mechanical properties. Ti–6Al–4V alloys require more improvement. For this purpose, there is an increasing interest to find new surface treatments, which provide titanium alloys to maintain their mechanical properties in the hard conditions and high temperatures during service.

On the other hand, niobium effects have been reported in the literature. The influence of niobium addition on mechanical characterization of steels [18, 19], ductile iron [20], Ni–19Si- based alloys [21], and pure magnesium [22] were studied. In addition, the diffusion of niobium on the surface of titanium and titanium alloys was documented [23, 24]. Many methods could be used in order to enhance the mechanical characterization of titanium alloys. Boriding treatment for titanium alloys was also performed, as mentioned before [11 - 14]. However, there is no study carried out to compare the diffusion of niobium and boride layers together on titanium alloy.

In this study, two stages were carried out by the diffusion of niobium after boriding treatment. The obtained microstructure was revealed using optical microscopy and Scanning Electron Microscopy. The phases produced on the surface of Ti-6Al-4V alloy were confirmed by X-ray diffraction. Furthermore, the mechanical properties such as micro hardness of nio-boride layers produced on titanium alloy Ti–6Al–4V were measured. In addition, the fracture toughness of niobized layers was determined. The aim of this work is to obtain a new treated titanium alloy by the diffusion of niobium and boron into the substrate of titanium alloy Ti-6Al-4V. The effect of niobium on the obtained microstructure, mechanical properties; especially microhardness of treated Ti-6Al-4V alloy was estimated. The two-stages, which consist of the diffusion of boron and niobium, caused the production of niobized layers can decrease the brittleness. Therefore, the influence of niobium content on micro hardness, and the modification of niobized layers on the microstructure were investigated and discussed in detail. Consequently, this work has developed a new coating on titanium alloy and improved its mechanical characterization, increased the micro hardness, strength of the titanium alloy, and increased its fracture toughness. For the first time, the microstructure and some mechanical properties of niobized titanium alloy Ti-6Al-4V were investigated in the present work.

EXPERIMENTAL

The Ti-6Al-4V-alloy was selected as the substrate for the thermochemical treatment. The chemical composition of the used alloy measured by X-ray fluorescence (XRF) spectrometry is shown in Table 1.

Niobizing treatment

Before treatment, the samples were cut in dimensions of 10 mm x 10 mm, and ground up to 1200 grid emery paper, and then washed ultrasonically bath in acetone

Table 1. XRF results and chemical composition of the Ti-6Al-4V-alloy.

Element	Al	V	Fe	O	C	Ti
wt.%	6.13	3.99	0.22	0.18	0.04	Balance

for 15 min. The first treatment carried out using Ekabor II (composed of 5 % B_4C, 5 % $NaBF_4$ and 90 % SiC) [12, 25]. The treatment was carried out at 950°C for 6 h with placing the samples in an electric resistance furnace. The powders mixture used for the second treatment was composed of a mixture of 60 % pure Nb, 20 % NH_4Cl and 20 % Al_2O_3 and was treated at 1000°C for 3 h, under argon atmosphere. After the treatment, the specimens were cooled in the furnace.

Metallographic and microstructure observations

Electrodeposited copper film was used to protect the produced coating during the metallographic preparation. For metallographic analysis, specimens were wet ground with SiC abrasive paper up to 4000. Specimens were polished with Al_2O_3, sectioned, and etched with Kroll's reagent with a solution of 5 vol. % (10 mL). The microstructure and morphology of niobized layers were performed by using the Leica DM6000 Microscope and Scanning Electron Microscope Tescan MIRA3 coupled with Energy-Dispersive X-ray Spectroscopy (EDS). The phase composition of the obtained coatings was investigated by using a Philips X'PERT MPD-30. X-ray diffraction (XRD) patterns of the surfaces of the specimens were obtained using a diffractometer equipped with a Cu K_α 1 radiation source (λ = 1.5418 Å). The diffractometer operated at 40 kV, 30 mA. Step scans for phase identification were achieved from θ - 4θ (20 to 80°) and a dwell time of 2 s at each position. The phases were identified through comparison with simulated diffraction patterns.

Indentation test

To evaluate the mechanical properties of the treated titanium alloy, compressive and micro hardness tests were conducted. Microhardness measurements and fracture toughness were achieved in a cross-section of the treated sample. The indentation tests were achieved by using a Vickers indentation tester under a charge of 100 g and a dwell time of 10 s on the longitudinal section. During the measurements, the indentation charge *F* and penetration depth *d* were increasingly noted. It was used for examinations at different distances from the sample to the substrate. The microhardness values were the average of at least 10 measurements. More details about the experimental procedure used for indentation as well as the equations used for calculating the fracture toughness were presented in the previous paper [6]. The investigated areas contained titanium niobized, and a mixture of titanium boride and niobium.

Fracture toughness

Agreeing to the literature data, different predictable approaches could be used for measuring fracture toughness. Nevertheless, the most popular technique used to evaluate the fracture toughness of surface layers is Vickers Indentation due to its efficiency and simplicity. Furthermore, in the case of the surface layer, this technique is recognized to be practically with acceptable accuracy [27].

The purpose of the fracture toughness studies is to determine the effect of niobium on the brittleness of the boride layer produced on Ti-6Al-4V alloy. Hence, the measurements were achieved in the area, that contained only the boride layer and then in the area containing the niobium layer. The fracture toughness was estimated in the etched cross-section of the niobized sample in order to find the area of investigation. For fracture toughness evaluation, the standard Vickers method of microhardness measurements was used. The Vickers indentation tests were achieved by using Mitutoyo device. In respect of determining the type of crack mode (Palmqvist, median, or intermediate), the different indentation loads were applied. The indentation Vickers and fracture toughness were measured using a load of 100 g.f (0.981 N). Ten measurements were achieved for both layers located in the niobized layer. The procedure explaining the measurements of microhardness and fracture toughness was reported in the reference [28]. Thus, the fracture toughness was evaluated by using equation (1), where a half-crack length (*C*) was measured by optical microscopy:

$$K_c = 0.028\left(\frac{E}{H}\right)^{\frac{1}{2}}\left(\frac{P}{C^{\frac{3}{2}}}\right) \quad (1)$$

where *H* is the Vickers micro hardness of the phase. *P* and *C* are the load and half of the indentation crack length, respectively. Many authors proposed the determination of a cracking mode (Palmqvist, intermediate, or radial-median) [18, 28].

Through fracture toughness measurements, the indentation and the resulting cracks should be far from the corners and edges of samples. It is preferable to move far enough about 500 μm between each indentation. The

lengths of diagonal (2a) and those of generated cracks (l) were measured by using an optical microscope equipped with a digital camera and computer. To determine the fracture toughness value, the calculation is based first on determining the coefficients according to the average crack mode. Then it depends on applying the aforementioned mathematical equation to obtain the values of fracture toughness *Kc* using the exact hardness values when loading 100 gf [6, 28].

Consequently, it should be well-known that the microstructure of the niobized layers with Vickers indentation produced crack were detected using Scanning Electron Microscope (SEM) and an optical microscope (OM). The concentrations of elements Ti, Al, V, B, and Ni in the investigated areas were determined using the X-ray micro analyzer equipped with EDS.

RESULTS AND DISCUSSION

Microstructure of the niobized layer

In the previous studies, the phase composition of the boride layer produced on Ti-6Al-4V alloy was already reported [11 - 14] when applying the boriding treatment. In the present work, niobized layers were obtained and have three different regions:

i) the outer region contained a niobium layer produced on the surface of Ti-6Al-4V-alloy;
ii) a dark grey region, which was identified as TiB_2/TiB layer between the niobium layer and matrix;
iii) the substrate titanium Ti-6Al-4V-alloy.

The niobized layers (both layers) reached a thickness of 345 μm. There was an intermediate layer between the coating and the matrix. It is noted that the microstructure of Ti64Al alloy after treatment of niobizing (via substitutional diffusion) in an inert argon medium consists of:

- formation of a continuous bright layer with a thickness of 50 to 90 μm with a microstructure containing the β phase due to saturation with Nb as shown in the optical micrograph of Fig. 1;
- intermediate zone made up of the β phase with fine grain size;
- dominant lamellar microstructure of the α'' phase at a different orientation, forming a smooth and compact morphology just after the intermediate zone towards the inside of the substrate with the presence of β phase in the grain boundaries.

The microstructure presented in Fig. 1 was preponderant in the boride layers produced on the Ti-6Al-4V-alloy. However, in the outer layer, an increase in the niobium concentration was detected. While in the second treatment, the niobium reacted with boron to form niobium boride phase beside titanium borides. The average thickness of the niobized layer was about 38 μm whereas the outer layer containing titanium boride has a depth of 210 μm. The cross-section of the niobized layer, and the interfaces TiB_2–TiB and TiB–NbB revealed a smooth and compact morphology. The niobized layers produced on the titanium Ti-6Al-4V alloy were smooth, homogeneous, and compact.

In this study, the niobized layers produced were thinner than that of the other thermo reactive deposition coatings, such as vanadium boride, titanium nitride, nitro-chroming, and vanadium carbide [11, 14, 30 - 35].

Increasing the diffusion temperature accelerates the diffusion process of boron and niobium in the titanium alloy, accelerated kinetics of titanium boride (TiB) layer formation on titanium surfaces during solid-state boron diffusion at very low temperatures [6, 7, 13, 15, 28, 37]. By comparing the variations of rolled strips with and without boron and titanium addition, the effect of boron on the mechanical characteristics of niobium on substrate was explored. It should be noted that the diffusion of boron in titanium is far faster than that of niobium in titanium alloy. Indeed, for the same treatment at 1100

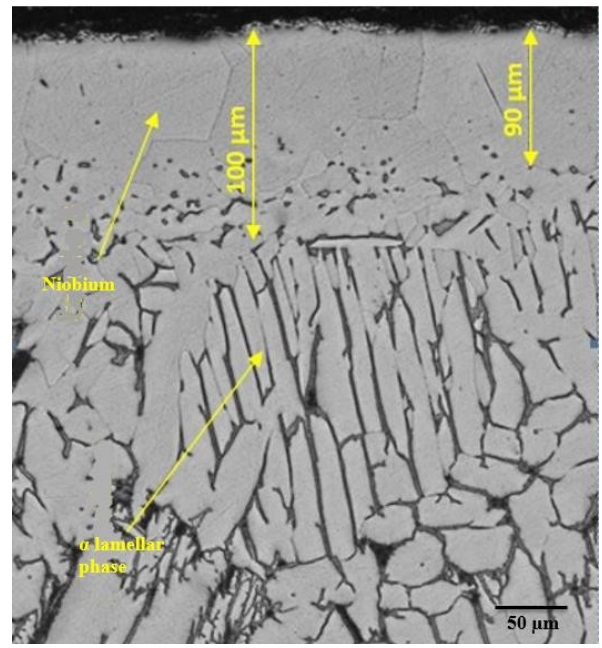

Fig. 1. Optical micrograph of Ti-6Al-4V-alloy treated.

°C, it has been recorded that a diffusion depth was equal to 287.79 μm [6, 28] and it was only 56.12 μm for Nb in titanium alloy.

In our previous studies [6] the thicknesses of boride layer were estimated by scanning electron microscopy and an optical microscope. The boride layer thickness values developed depending on the boriding temperature and time. In addition, the boride layer thickness of steel augmented dramatically with microwave heating which evidently result in cost saving due to lower temperature and shorter processing time.

According to the literature, the least thick of boride layer is affected by salt bath process for AISI 8620 steel and ferro-niobium, ammonium chloride + alumina medium for AISI 1040 steel, respectively [30 - 32]. However, the thickest boride layer is obtained by titanium nitride + aluminum chromium nitride + aluminum oxide medium for AISI 4140 steel [34]. The highest micro hardness value was obtained for molten borax and chromium powder for CK45 steel, as seen in Table 2. It should be noted that the large thickness of boride layer, may affect the ignited parts, especially those used for engines and where there are frictions.

The XRD analysis of the niobized layer confirmed the presence of boride phases (TiB_2 and TiB) and a niobium boride phase (NbB) as shown in Fig. 2. The layers produced on the surface of the titanium alloy are rich in niobium with the formation of the NbB phase. This result was confirmed by XRD analysis. The niobium concentration in the outer layer is much higher than that in the inner part of the layer, which was confirmed by XRD and EDS analyses, as shown in Fig. 2 and Fig. 3,

Table 2. Comparison between niobized Ti-6Al-4V-alloy and other steel treated.

Substrate	Treatment	Phases obtained	Thickness (μm)	Hardness (HV)	Reference
AISI 8620 steel	Salt bath, vanadium	FeB + FeB, and VB + V_2B_3	3 to 25	-	30
AISI 1010 steel	nitro-chromizing 575°C for 2 h, ferro-chromium, ammonium chloride and alumina at 1000°C for 1-4 h	Cr_2N, FeCr	5.16 to 13.45	1789 HV	31
AISI 1040 steel	ferro-niobium, ammonium chloride and alumina at 1073, 1173 and 1273 K for 1 - 4 h	NbC and Nb_2C	3.42 to 11.78	1792 HV	32
aluminium	laser-treated and sol-gel aluminum nitride & laser processing	Al_2O_3,$CaCo_3$, MgO	6	-	33
cutting tools	TiN, $Al_2O_3$and Ti(C,N)	TiN, Al_2O_3 and Ti(C,N)	11.5	1150 and 1650	32
AISI1025 steel H1 based ceramic	mixture of TiO_2,SiO_2, hBN and graphite powders, 5 min at 100°C in argon	TiB_2, TiN, SiC and hBN	-	14 - 22 GPa	32
pure iron	Ekaboor 950°C for 6 h nitride cyanamide and calcium silicate 550°C for 6 h	Fe3N,FeB, Fe2B	120 to 240 boride + nitride	-	33
AISI 4140 steel	e machining hard turning	Titanium nitride+ aluminium chromium nitride coated WC/Co and aluminum oxide	200		34
CK45 steel	molten borax & Chromium powder + Cr_2O_3 powder and V_2O_5 powder 1000°C for 14 h	chromium and Vanadium carbide ($Cr_{23}C_6$,Cr_7C_3), and Vanadium carbide (V_8C_7)	6	3500	35
Ti-6Al-4Valloy	Ekabor 950°C/3h + niobium 1100°C/3h	TiB_2, TiB and NbB	287+56	1728	This work

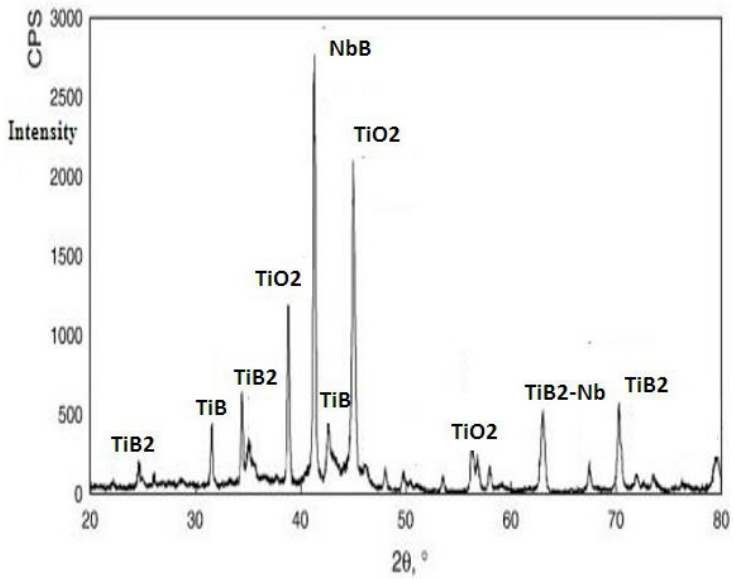

Fig. 2. XRD analysis of the niobized phases.

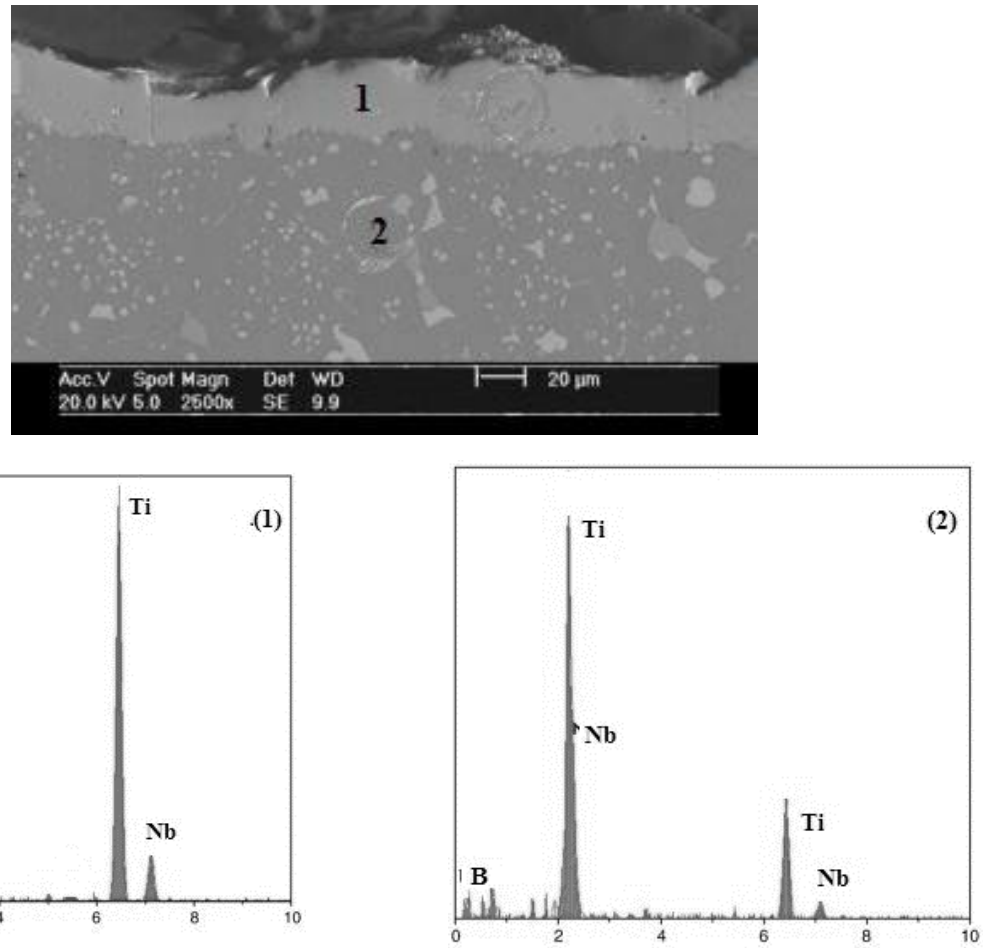

Fig. 3. SEM micrograph of titanium Ti-6Al-4V-alloy treated and EDS analysis.

respectively. However, phases consisting of boron and niobium at the same time were not identified. This may have happened because of the fact that those phases were produced in two different layers below the surface of the sample. In order to detect the distribution of titanium and niobium in the cross-section of the niobized layer, X-ray spectroscopy (EDS) was also carried out. The phases present in the niobized layers produced on titanium Ti-6Al-4V alloy were shown in Fig. 3. The presence of a minor concentration of the niobium element was confirmed by EDS analysis.

Mechanical properties

The results of indentation measurements, obtained along the two layers of the cross-sections of treated samples (the niobized and boride layers) were presented in Table 3. Ten Vickers indentations were then achieved in the niobized and boride layers produced on the Ti-6Al-4V alloy. The ten measurements were carried out in both layers. The presence of niobium in the outer layers powerfully increased the values of Vickers microhardness. The indentation was achieved in the outer layer, and it was characterized by a higher hardness value (1728 ± 50 HV) [29].

Thus, the presence of niobium in the outer layer was the reason for the improvement in the mechanical properties. It is known that the micro hardness of the niobized layer after boriding treatment was higher than the boride layer. According to the literature data, the phases, TiB_2 and TiB, did not present different micro hardness values [11 - 14].

Table 3 reveals the results of measurements using the indenter for the niobized Ti-6Al-4V-alloy. Therefore, Vickers indentation and fracture toughness were measured in a metallographic cross-section of the niobized layers produced on Ti-6Al-4V alloy.

Those layers contained two layers, which differed in the phase composition. The presence of boride niobium (NbB) was established only in the outer layer, while the inner layer was composed of TiB_2 and TiB. The latter did not contain any niobium. α”-type titanium alloy has a higher micro hardness than α phase in the non-treated alloy, it has good cold-forming ability and strength. Hence, a new type of coating titanium alloy was found with a nontoxic α” + β stable element, this alloy has been extensively used in the next generation of biomedical implants to replace the widely used titanium α” + β type alloy. Typically, materials during indentation can indicate one of two types of behavior: elastic or plastic. All the indentations generated in the niobized layer were characterized by complex elastic-plastic behavior. However, lower values were calculated for the inner layer, in which only titanium borides appeared. The indentation marks, obtained in the outer layer, were observed due to the presence of niobium in this layer, which caused this area to be somewhat more prone to

Table 3. Results of measurements using the indenter for the niobized Ti-6Al-4V-alloy.

Tested area	Indentation number	HV
Niobized layer	1	1728 ± 50
	2	1666 ± 43
	3	1649 ± 37
	4	1636 ± 12
	5	1695 ± 25
Boride layer	6	1696 ± 38
	7	1656 ± 24
	8	1336 ± 12
	9	866 ± 10
	10	096 ± 15

plastic deformation during indentation in comparison to the compact titanium borides layer. In the previous studies the mechanical properties were measured for the boride layer produced on titanium alloy [6, 13, 14]. This boride layer contained titanium borides (TiB_2 and TiB) and was characterized by an average indentation hardness of 1500 HV.

In the present study, similar values were obtained for the outer layer - average hardness of 1728 ± 50. Obviously, the same phase composition of both layers was the reason for similar results.

To measure the fracture toughness, it is sufficient to create a crack and to subsequently load the test sample until it breaks. The fracture toughness is quantified by the critical stress intensity factor K_c [29]. Several techniques have been used to evaluate the fracture toughness of the substrates and coated samples, and each of them is based on pre-cracking of the sample by applying a force through loading. A Vickers indentation is used as a simple technique for assessing toughness by shouting a Vickers indentation. Several equations have been proposed in the literature [29, 36 - 38]. Generally, they take into account the following factors:

iv) modulus,
v) hardness,
vi) dimensions of the indentation, and cracks.

There are three types of crack modes that can describe the materials: radial-median [36, 24], Palmqvist [11, 25, 26], or intermediate [18]. These crack modes changed their top-view and cross-section profiles. The different types of cracks occur during an indentation. The type of cracking depends on the shape of the indenter, the type of material, and the applied load. Generally, a spherical indenter generates a conical crack.

On the other hand, a pointed Vickers indenter leads to median/radial or lateral cracks. The combination of these cracks leads to cracking profiles of the median/radial or palmqvist type. Some studies have already been done [26, 36, 39] showing that the resistance to crack initiation has no clear relationship with the mechanical properties (Kc, H, etc.), but rather with the residual stresses that can be reduced. The use of each mode for the calculation of fracture toughness needed an explanation. The technique used in order to define the crack mode was designated in the literature [28, 40]. Clearly, the phase composition of niobized layers powerfully inclined its fracture toughness. The niobized layers containing niobium, have a negative influence on the brittleness.

Vickers microhardness (HV) and fracture toughness (K_c) values from the indentation in the niobized layer and that of the boride layer produced on Ti-6Al-4V alloy were presented in Table 4. The indentations of the cracks were also evident in the perpendicular direction (90°) to the surface. The average fracture toughness in $0^o/90^o$ orientated samples was less than that of specimens with zero-degree orientations. Samples have less flexural strength than (0^o) and (90^o), which is consistent with the results in Table 4. The fracture toughness values K_c were about 35 % lower than those obtained in the borided layer. The presence of niobized layers produced a significant diminution of fracture toughness. In order to decide the effect of niobium on the fracture toughness of the niobized layer produced on Ti-6Al-4V alloy, investigations were also achieved in the inner layer, which conducted titanium borides (TiB_2, TiB), and niobium boride (NbB). These results showed a minor anisotropy of fracture toughness measured in the inner layer, which included only the boride layers. The brittleness of the niobized layer is contingent on its phase composition. In the present study, titanium borides (TiB_2 and TiB) were produced on the Ti-6Al-4V-alloy. The distinct toughness measurements were conducted for individual phases, i.e. TiB_2, TiB, and NbB. Fracture toughness values were very low compared to the reported values [28, 29, 40].

Those factors and any pre-existing residual stresses influence this parameter. In this case, for the estimate of the brittle strength of a non-uniform niobized layer, it is desirable to use the critical stress intensity factors offered in the form of the function $K_c(\theta)$, where $0^\circ \leq \theta \leq 90^\circ$ is the coordinate angle between the direction of cracks propagation and the surface. Hence, it is essential to express brittle fracture standards in the niobized layers for evaluating the facture toughness Kc [39, 40].

Table 4 regrouped the results of ten measurements found for this layer. The cracks were generated mostly in the direction parallel (0°) to the surface. Nevertheless, in the case of some indentations, the cracks were also obvious in the perpendicular direction (90°) to the surface. These results show that the presence of niobium produced 0 reduction in fracture toughness in comparison with the outer layer, which did not contain niobium [28, 29, 39, 40].

Table 4. Vickers micro hardness (HV) and fracture toughness (Kc) values from the indentation in the niobium layer and boride layer produced on titanium Ti-6Al-4V-alloy.

Code	Direction of crack propagation	Niobnium layer		boride layer	
		HV	Kc ($MPa \cdot m^{1/2}$)	HV	Kc ($MPa \cdot m^{1/2}$)
1	0°	1728 ± 50	1.55 ± 0.54	1696 ± 38	4.42 ± 0.60
	90°		2.02 ± 0.56		3.74 ± 0.05
2	0°	1668 ± 43	2.76 ± 0.45	1656 ± 24	3.20 ± 0.21
	90°		1.78 ± 0.56		2.94 ± 1.83
3	0°	1649 ± 37	1.81 ± 0.35	1336 ± 12	4.15 ± 1.35
	90°		2.07 ± 0.46		2.18 ± 1.36
4	0°	1636 ± 12	1.99 ± 0.23	866 ± 10	2.05 ± 4.08
	90°		1.27 ± 0.35		2.22 ± 3.47
5	0°	1695 ± 25	0.82 ± 0.44	960 ± 15	1.37 ± 2.22
	90°		1.98 ± 0.35		1.47 ± 0.95
6	0°	1712 ± 36	1.78 ± 0.33	1706 ± 24	4.14 ± 0.62
	90°		2.23 ± 0.12		3.04 ± 0.18
7	0°	1658 ± 25	2.84 ± 0.23	1666 ± 38	3.45 ± 0.36
	90°		1.89 ± 0.41		2.87 ± 1.66
8	0°	1625 ± 23	1.99 ± 0.52	1342 ± 22	3.55 ± 1.40
	90°		1.87 ± 0.25		2.11 ± 1.22
9	0°	1612 ± 15	1.81 ± 0.34	840 ± 22	2.34 ± 2.25
	90°		1.33 ± 0.42		2.68 ± 2.35
10	0°	1688 ± 12	0.92 ± 0.53	210 ± 17	1.50 ± 2.16
	90°		2.12 ± 0.60		1.66 ± 1.12

CONCLUSIONS

In this study, the niobizing process was carried out on Ti-6Al-4V alloy. The microstructure and mechanical properties of the niobized layers produced were investigated. Based on the results obtained, the following conclusions can be drawn as follows:

- Boron diffused at the surface of the Ti-6Al-4V alloy in the first treatment, forming boride layers. In the second step, the boride samples were treated in a power mixture rich in niobium to produce niobized layers.
- The niobized layers are mainly composed of two different layers. The outer layer contained only boride niobium (NbB), while the inner contained the two titanium borides (TiB_2 and TiB). The microstructure of the produced coating on the titanium alloy was smooth and compact.
- The micro hardness measured in the zone of the niobized layer was significantly high and equal to $1728 \pm 50\ HV_{0.1}$.
- Fracture toughness values K_c were about 35% lower than those obtained in the titanium borides layer. The presence of niobium with boride layers produced a significant diminution of fracture toughness.
- The niobizing treatment could be the reason for the formation of niobized layers.
- There is an undesirable effect of niobium on the increased brittleness of titanium alloy.

Acknowledgements

This work has been supported by the Laboratory of Applied Sciences and Didactics at Ecole Normale

Supérieure de Laghouat under project code A24N01EN030120210001. The authors wish to thank DGRSDT of Algeria for the support of this work and "Plateforme d'analyses physico-chimiques" of Laghouat-Algeria. The authors would like also to thank Dr. Taieb Kabbache for his help.

REFERENCES

1. P.R. Jothi, K. Yubuta, B.P.T. Fokwa, A. Simple, General synthetic route toward nanoscale transition metal borides, Adv. Mater., 30, 2018, 1704181.
2. A.K Sinha, Boronizing. ASM Handbook, OH, USA, J. Heat Treat., 4, 1991, 437.
3. M. Kulka, Trends in Thermochemical Techniques of Boriding, Eng. Mater., 2019, 1612-1317.
4. G. Akopov, M.T. Yeung, R.B. Kaner, Rediscovering the crystal chemistry of borides, Adv. Mater., 29, 2017, 1604506.
5. H. Wan, X. Liu, M. Qing, Q. Peng, Y. Li, Surface structure and morphology evolution of iron borides under dynamic conditions: A theoretical study, Appl. Surf. Sci., 525, 2020, 146462.
6. A. Kaouka, O. Allaoui, M. Keddam, Growth kinetics of the boride layers produced on SAE 1035 steel, Matér. & Tech., 101, 2013, 705.
7. I. Campos-Silva, M. Ortiz-Domínguez, M. Keddam, N. López-Perrusquia, M. Elías- Espinosa Kinetics of the formation of Fe_2B layers in gray cast iron: Effects of boron concentration and boride incubation time, Appl. Surf.Sci., 255, 2009, 9290-9295.
8. X.B. Hu, Y.L. Zhu, X.L. Ma, Crystallographic account of nano-scaled intergrowth of M_2B-type borides in nickel-based super alloys, Acta Mater., 6815, 2014, 70-81.
9. Y.Z. Chen, S.W. Wei, K.J. Wu, Effect of promoter on selective hydrogenation of α, β- unsaturated aldehydes over cobalt borides, Appl. Cataly. A., 99, 1993, 85-96.
10. C. Petit, M.P. Pileni, Nanosize cobalt boride particles: Control of the size and properties, J. Magn. and Magn. Mater., 166, 1997, 82-90.
11. A. Kaouka, K.Benarous, Characterization and properties of boriding titanium Alloy Ti6Al4V, Acta Phys. Pol. A, 137, 2020, 493-495.
12. A. Kaouka, K. Benarous, Electrochemical boriding of titanium alloy Ti-6Al-4V, J. Mater. Res.and Techno., 8, 2019, 6407-6412.
13. N. Makuch, M. Kulka, M. Keddam, S. Taktak, P. Dziarski, Growth kinetics and some mechanical properties of two-phase boride layers produced on commercially pure titanium during plasma paste boriding, Thin Solid Films, 626, 2017, 25-37.
14. M. Keddam, S. Taktak, Characterization and diffusion model for the titanium boride layers formed on the Ti6Al4V alloy by plasma paste boriding, Appl. Surf. Sci., 399, 2017, 229-236.
15. L.G. Yu, X.J. Chen, K.A. Khor, G. Sundararajan, FeB/Fe_2B phase transformation during SPS pack-boriding: Boride layer growth kinetics, Acta Mater., 53, 2005, 2361-2368.
16. S. Taktak, Some mechanical properties of borided AISI H13 and 304 steels, Mater.& Design, 28, 2007, 1836-1843.
17. N. Makuch, Nanomechanical properties and fracture toughness of hard ceramic layer produced by gas boriding of Inconel 600 alloy, Trans; of Nonfer. Met. Soci. of China, 30; 2020; 428-448.
18. G. Beniwal, K. Saxena, Effect of niobium addition in grey cast iron: A short review Mater. Today: Proce., 26, 2020, 2337-2343.
19. S. Pan, F. Zeng, N. Su, Z. Xian, The effect of niobium addition on the microstructure and properties of cast iron used in cylinder head, J. Mater. Res. Technol., 9, 2020, 1509-1518.
20. J.S.C. Jang, C.H. Tsau, The effect of niobium additions on the fracture of Ni–19Si-based alloys, High Temp. Aluminides and Intermet., 1992, 525-531.
21. X. Chen, L. Zhao, W. Zhang, H. Mohrbacher, Q. Zhai, Effects of niobium alloying on microstructure, toughness and wear resistance of austempered ductile iron, Mater. Sci. and Eng. A, 7608, 2019, 186-194.
22. M. Shanthi, P. Jayaramanavar, V. Vyas, D.V.S. Seenivasan, M. Gupta, Effect of niobium particulate addition on the microstructure and mechanical properties of pure magnesium, J. Alloys and Comp., 5135, 2012, 202-207.
23. S. Divinski, F. Hisker, C. Klinkenberg, C. Herzig, Niobium and titanium diffusion in the high niobium-containing Ti–54Al–10Nb alloy, Intermetallics, 14, 2006, 792-799.
24. Z. He, Z. Wang, W. Wang, A. Fan, Z. Xu, Surface modification of titanium alloy by plasma niobium alloying process, Surf.and Coat. Techn., 201, 9–1126, 2007, 5705-5709.

25. I. Özbek, B.A. Konduk, C. Bindal, A.H. Ucisik, Characterization of borided AISI 316L stainless steel implant, Vacuum, 65, 2002, 521-525.
26. T. Takasugi, H. Kawai, Y. Kaneno, The effect of Cr addition on mechanical and chemical properties of Ni_3Si alloys, Mater. Sci. and Eng. A 329–331, 2002, 446-454.
27. D. Chicot, G. Duarte, A. Tricoteaux, B. Jorgowski, A. Lericheb, J. Lesage, Vickers Indentation Fracture (VIF) modeling to analyze multi-cracking toughness of titanium, alumina and zirconia plasma sprayed coatings, Mater. Sci. and Eng.: A 527, 2009, 65-76.
28. A. Kaouka, O. Allaoui, M. Keddam, Properties of boride layer on boride SAE 1035 steel by molten salt, Appl. Mech.l Mater., 467, 2014, 116-121.
29. I. Campos, R. Rosas, U. Figueroa, C. VillaVelazquez, A. Meneses, A. Guevara, Fracture toughness evaluation using Palmqvist crack models on AISI 1045 borided steels, J. Mater.Sci. and Eng. A, 488, 2008, 562-568.
30. S. Sen, The characterization of vanadium boride coatings on AISI 8620 steel, Surf.&Coat. Techno., 190, 2005, 1-6.
31. O. Ozdemir, S. Sen, U. Sen, Formation of chromium nitride layers on AISI 1010 steel by nitro-chromizing treatment, Vacuum, 81, 2007, 567-570.
32. B.S. Yilbas, H. Ali, N. Al-Aqeeli, M.M. Oubaha, N. Abu-Dheir, Laser gas assisted nitriding and sol–gel coating of alumina surfaces: Effect of environmental dust on surfaces, Surf. and Coat. Techno., 28915, 2016, 11-22.
33. O.A. Gómez-Vargas, J. Solis-Romero, U. Figueroa-López, M. Ortiz-Domínguez, J. Oseguera-Peña, A. Neville, Boro-nitriding coating on pure iron by powder-pack boriding and nitriding processes, Mater. Letters, 176, 2016, 261-264.
34. D. Misra, B. Dhakar, E.Anusha, S.M.Shariff, S. Mukhopadhyay, S. Chatterjee, Evaluation of nanomechanical and tribological properties of laser surface alloyed boride-nitride-carbide ceramic matrix composite coatings, Ceramics Inter., 44, 2018, 17050-17061.
35. A. Ghadi, M. Soltanieh, H. Saghafian, Z.Yang, Investigation of chromium and vanadium carbide composite coatings on CK45 steel by Thermal Reactive Diffusion, Surf. and Coat. Technol., 28915, 2016, 1-10.
36. I. Ozbek, C. Bindal, Mechanical properties of boronized AISI W4 steel, Surf. and Coat. Technol., 154 (2002) 14-20.
37. G. Kara, G. Purcek, Growth kinetics and mechanical characterization of boride layers produced on β-type Ti-45Nb alloy, Surf. and Coat. Technol., 35225, 2018, 201-212.
38. V. Shahedifar, M. Ghassemi Kakroudi, H. R. Baharvandi, F. Rezaei, Investigation of strength, fracture toughness, and crack propagation pattern of TaC-based fibrous monoliths as a function of microstructure architecture, International J. of Ref. Metals and Hard Mater., 78, 2019, 332-339.
39. Y. Kato, H. Yamazaki, S. Yoshida, J. Matsuoka, Indentation cracking of glass Part I: Load-dependence of deformation during Vickers indentation test., XXI-st International congress on glass, Strasbourg, 1-6 july 2007.
40. I. Campos-Silva, M. Flores-Jiménez, G. Rodríguez-Castro, E. Hernández-Sánchez, J. Martínez-Trinidad, R. Tadeo-Rosas, Improved fracture toughness of boride coating developed with a diffusion annealing process, Surf. and Coat. Techno., 237, 2013, 429-439.